Lipids
DOI 10.1007/s11745-014-3945-0

ORIGINAL ARTICLE

GC-EI-MS Analysis of Fatty Acid Composition in Brain and Serum of Twitcher Mouse

Assunta Zanfini · Elena Dreassi · Anna Berardi · Paola Piomboni · Elvira Costantino-Ceccarini · Alice Luddi

Received: 27 March 2014 / Accepted: 21 August 2014

Abstract Globoid cell leukodystrophy or Krabbe disease is an inherited autosomal recessive disorder caused by mutations in the galactosylceramidase gene. The objective of the study was to present information about the fatty acid (FA) composition of the brain and serum of twitcher mice, a mouse model of Krabbe disease, compared to wild type, in order to identify biomarker of disease progression. We defined the FA profiles by identifying the main components present in serum and brain using GC-EI-MS analysis. The FA percentage composition was measured and data were analyzed considering the disease and the mouse age as experimental factors. Significant correlations were established, both in brain and in serum, in the fatty acid percentage composition of twitcher compared to wild type mice. The most abundant saturated fatty acid in brain was the palmitic acid (C16:0) with mean values significantly increased in twitcher mouse ($p = 0.0142$); moreover, three monounsaturated, three polyunsaturated (PUFA) and a plasmalogen were significantly correlated to disease. In the serum highly significant differences were observed between the two groups for three polyunsaturated fatty acids. In fact, the docosahexaenoic acid (C22:6n3c) content was significantly increased ($p = 0.0116$), while the C20 PUFA (C20:3n6c and C20:5n3c) were significantly decreased in twitcher serum samples. Our study shows a specific FA profile that may help to define a possible pattern that could distinguish between twitcher and wild type; these data are likely to provide insight in the identification of new biomarkers to monitor the disease progression and thereby permit the critical analysis of therapeutic approaches.

Keywords Fatty acids · Monounsaturated fatty acids · Polyunsaturated fatty acids · Twitcher mouse · Brain · Serum

Abbreviation

MUFA	Monounsaturated fatty acid(s)
PUFA	Polyunsaturated fatty acid(s)
GLD	Globoid cell leukodystrophy
GALC	Galactosylceramidase
CNS	Central nervous system
PNS	Peripheral nervous system
DHA	Docosahexaenoic acid
FAME	Fatty acid methyl ester(s)
FID	Flame ionization detection
FA	Fatty acid(s)
DMA	Dimethyl acetals

Introduction

Globoid cell leukodystrophy (GLD), also known as Krabbe disease, is an inherited autosomal recessive disorder caused by mutations in the galactosylceramidase (GALC) gene. GALC is a lysosomal enzyme essential for normal catabolism of galactolipids, including a major myelin component, galactosylceramide, and psychosine [1]. The characteristic biochemical feature of Krabbe disease is the

A. Zanfini · E. Dreassi
Department of Biotechnology, Chemistry and Pharmacy, University of Siena, Viale Bracci, 53100 Siena, Italy

A. Berardi · P. Piomboni · E. Costantino-Ceccarini · A. Luddi (✉)
Department of Molecular Medicine and Development, University of Siena, Viale Bracci, 53100 Siena, Italy
e-mail: aliceluddi@gmail.com; luddi@unisi.it

Published online: 11 September 2014

lack of accumulation of the undegraded galactosylceramide in the brain, explained by the early degeneration of the myelin forming cells and the block in the synthesis of galactosylceramide [2, 3]. In fact, GALC deficiency results in abnormal accumulation of psychosine, a toxic metabolite which has been demonstrated to induce apoptotic death in oligodendrocytes and Schwann cells throughout respectively the central nervous system (CNS) and peripheral nervous system (PNS) [4, 5]. To date, several therapeutical approaches have been fully explored in the twitcher mouse, the murine model of Krabbe disease [6–8], as well as in humans [9, 10], however, there is no currently available therapy for GLD or a biomarker that specifically measures disease progression and therapy effectiveness. Hence, the identification of biomarkers for Krabbe disease would help follow up any potential new therapeutic approaches. Metabolomics can provide a useful support in the search for biomarkers, since it assesses the end products of gene expression and environmental influences along the pathway. Based on multivariate analysis of complex biological profiles, metabolomics has been successfully applied to many fields such as disease diagnosis [11, 12], biomarker screening [13] and characterization of biological pathways [14]. Metabolomic targeted profiling involves the profiling of selected metabolites in different physiological states [15]. Fatty acids (FA) are key bioactive molecules in living organisms contributing to various cell functions like energy storage or signal transduction. They are precursors of eicosanoids, prostaglandins and leukotrienes, and are also main constituents of lipids that account for about 50–70 % of the dry weight of both the human brain and myelin, respectively [16, 17]. Much of the structure and function of myelin is dependent on its lipid content, thus lipids may be used as markers for myelin membrane integrity and associated nerve fiber function. The observation that abnormal FA composition may have a role in myelin abnormalities in the brain is supported by the evidence that alteration in polyunsaturated fatty acids (PUFA) content is correlated to brain pathologies [18, 19]. Plasmalogens are important lipids, especially during myelinogenesis of the brain [20]. A fatal congenital disease, Zellweger's syndrome, is characterized by a decrease in plasmalogens [21], which appears to parallel that in DHA [22].

There is little information on the fatty acid composition of twitcher brain. Most insights are related to the galactolipid composition of the brain. Igisu et al. [23] reported a slight reduction in total lipid towards the terminal stage of disease in addition to an abnormal concentration of galactolipids galactosylceramide and sulfatide. Galactosylceramide was decreased at 37 and 42 days whereas the decrease in sulfatide occurred earlier, namely from 25 days, resulting in an increased ratio of galactosylceramide to sulfatide [23]. More recent data have shown that there is a significant decrease in long chain fatty acids and an increase in shorter chain fatty acids in galactosylceramides and ceramides from twitcher mice compared with control mice. These changes may be related to the demyelination characteristic of twitcher mouse [24].

Gas chromatographic analysis is the analytical technique typically used for fatty acid (FA) analysis. This technique has been largely employed to analyze FA in various matrices such as cell membranes, plasma, tissues, etc. [25, 26]. The FA analysis by GC–MS is a very useful approach, successfully used for their detection in biological samples [27–30].

In this study we investigated the FA composition in the brain and serum of twitcher mice. We defined the FA profiles by identifying the main components present in serum and brain using GC-EI-MS analysis. The FA percentage composition was also measured and possible significant differences between twitcher and control mice were checked. Statistical classification models were applied to the class separation of twitcher mice and controls. Discriminate FA that could distinguish between the two groups were checked.

This allowed the identification of key FA, or a FA ratio, that could distinguish between the twitcher and the wild type, probably providing potential biomarkers for monitoring the disease progression and thereby permitting critical analysis of therapeutic approaches.

Materials and Methods

Reagents and Standards

Fatty acid standards: nonanoic acid (C9:0), C9:0 methyl ester, myristic acid (C14:0), palmitic acid (C16:0), palmitoleic acid (C16:1n-7), stearic acid (C18:0), oleic acid (C18:1n-9), linoleic acid (C18:2n-6), linolenic acid (C18:3n-3), γ-linolenic acid (C18:3n-6), *cis*-11,14-eicosadienoic acid (C20:2n-6), arachidonic acid (C20:4n-6), *cis*-5,8,11,14,17-eicosapentaenoic acid (C20:5n-3), *cis*-4,7,10,13,16,19-docosahexaenoic acid (C22:6n-3), tetracosanoic acid (C24:0), selacholeic acid (C24:1n-9) and Supelco® 37 Component FAME Mix were purchased from Sigma–Aldrich S.r.l (Milan, Italy). All solvents and reagents used for sample preparation were from Merck (Darmstadt, Germany). Milli-Q quality water (Millipore, Milford, MA, USA) was used. The BF3 14 % methanolic solution was from Sigma–Aldrich S.r.l (Milan, Italy).

Experimental Animals: Mouse Serum and Brain Samples

Heterozygous twitcher (GALC±) mice on a congenic C57BLJ/6 background were originally obtained from The

Jackson Laboratory (Bar Harbor, ME). Animals were maintained under standard housing conditions with free access to food and water. All animal procedures were conducted in conformity with Public Health Ser-vice (PHS) Policy on Humane Care and Use of Laboratory Animals. Animal experimentation policy was approved by the Local Ethical Committee of the University of Siena. Heterozygous mice (GAL C±) were mated to obtain homozygous twitcher (GALC−/−) or homozygous wild type (GALC+/+) mice. Genotypes of newborn pups were identified by PCR for the twitcher mutation [31]. At the age of 25 or 35 days, animals were killed by lethal injection of phenobarbital. Serum and brain tissue were collected and stored at −20 °C.

Sample Preparation

Lipid extraction from brain tissue was carried using the Bligh and Dyer method [32] with minor modifications. Each sample (200 mg) was placed in a glass–glass Dounce homogenizer, combined with 3 mL of CH_2Cl_2:CH_3OH mixture (1:2 v/v) containing a fixed amount of nonanoic acid C9:0 (internal standard, IS) and homogenized for 2 min. To the extraction mixture was added butylated hydroxytoluene (BHT 100 μM) to inhibit lipid peroxidation. One mL of CH_2Cl_2 and 1 mL of distilled water were added to each extract and the resulting mixture was stirred for 30 s. After filtration, the sample was centrifuged at 4,000 rpm for 5 min. The CH_2Cl_2 layer was separated, dried under nitrogen, reconstituted in 1 mL of *n*-hexane and then used for fatty acid analysis. The FAME were obtained with 14 % BF_3 methanolic solution according to the method of Morrison and Smith [33] The sample was maintained at 90 °C for 1 h and then, after cooling, extracted twice with 500 μL of *n*-hexane. After centrifugation at 4,000 rpm for 5 min, the *n*-hexane phases were collected, evaporated under nitrogen and then redissolved in 500 μL of *n*-hexane.

Serum analysis was carried out using a previously published method with minor modifications [34]. Briefly, 100 μl serum aliquots (containing a fixed amount of C9:0 methyl ester, IS and of BHT 100 μM) were spiked with 500 μL of 0.4 M KOH-CH_3OH solution. The sample was vortexed for 30 s and placed at room temperature for 10 min. FAME extraction was performed using *n*-hexane (500 μL of *n*-hexane added twice). The *n*-hexane phases were separated after centrifugation at 4,000 rpm for 5 min and dried by evaporation under N_2 gas. Prior to GC–MS analysis the sample was reconstituted in 500 μL of *n*-hexane.

GC–MS Analysis

The analysis was carried out using a gas chromatograph VARIAN 3900 with CP-8400 auto injector coupled to an ion-trap mass spectrometer (VARIAN Saturn 2000 MS–MS). A SPTM-2380 fused silica capillary column (60 m × 0.25 mm I.D., 0.2 μm film thickness) provided by Supelco (Bellefonte, PA, USA) was used. Oven temperature was programmed from 100 to 240 °C at 10 °C/min and then increased to 260 at 5 °C/min; finally, the oven was maintained at 260 °C for 10 min. Injector temperature was set at 230 °C; 1 μL aliquots were injected and the split ratio of 1:10 was used. Helium was employed as carrier gas with a flow rate of 1 mL/min. The ion-trap mass spectrometer was operated in the electron impact ionization (EI) mode with a ionization voltage of 70 eV. The analyses were performed with a filament-multiplier delay of 9 min and data acquisition was carried out in the range *m*/*z* 50–650 in full scan mode. The transfer line was maintained at 250 °C, the manifold and trap temperatures were set at 80 and 150 °C, respectively. Instrument control and mass spectrometry data were managed by a personal computer running the Saturn GC–MS WorkStation software (6.30 version).

Identification of the chromatographic peaks was made by comparison of mass spectra with those provided by commercial standards and by comparing the retention times when they yield identical MS spectra. A comparison with National Institute of Standards and Technology (NIST) library was also performed.

The GC-FID analyses were carried out using a Chrompack CP 9001 GC equipped with a FID detector and a split/splitless injector. Injector and detector temperatures were set at 230 and 280 °C respectively. Helium was employed as carrier gas with a flow rate of 1 mL/min; 1 μL aliquots were injected and the split ratio of 1:10 was used. The fused silica capillary column and the oven temperature program described for GC–MS analysis were employed. Data acquisition was carried out using Perkin Elmer TotalChrom Navigator software v 6.3.1.

Statistical Analysis

All analyses were run in triplicate and data were expressed as means ± standard deviations (SD). A two-way analysis of variance (ANOVA) followed by Bonferroni's post hoc comparison test was performed. Data were analyzed considering the disease and the mouse age as experimental factors. Their possible interaction effect was also investigated. Differences were considered significant for *p* values

$\leq$0.05 at the 95.0 % confidence level. All calculations were performed using the Stat Graphics Plus Package (4.1.version).

Results

Optimization of Sample Preparation and GC-EI-MS Analysis

The aim of this preliminary step was to develop and optimize an analytical procedure useful for the analysis of fatty acids in brain tissue and serum. The methods conventionally employed for FA analysis in biological samples consist of several steps which include the extraction of the total lipid fraction, the conversion of all fatty acids into volatile compounds using various derivatization procedures and finally the analysis with GC.

In order to optimize the sample preparation procedure we considered both the amount of extracted lipids than the potential effect of the extraction procedure on degradation of the lipids and the fatty acid composition. In the present work the analysis of brain samples was performed using conventional methods with minor modifications, as described in the "Materials and Methods" section of this paper. The Bligh and Dyer method, which is routinely used for lipid extraction from tissues, was partly modified and used. As described by other authors, we found that methylene chloride give identical results to chloroform–methanol mixture, so that this solvent was preferred and used considering its lower toxicity [35]. The derivatization procedure which allows the conversion of FA into FAME was carried out using 14 % BF_3 methanolic solution [33]. The derivatization yield was evaluated at several time points (5, 15, 30, 60 min) at two different temperatures (60 and 90 °C). Maximum derivatization was obtained after 60 min at 90 °C. Using these experimental conditions, good recovery values were obtained for five FA standard solutions (C16:0, C18:0, C18:1n-9, C20:4n-6, C22:6n3) at 3 concentration levels. The relative standard deviation (RSD) calculated from the peak area was used to test the derivatization efficiency. The RSD ranged from 4.5 to 12 %. The recoveries of FA were tested at three concentration levels and the inter-sample reproducibility was between 80 and 110 %.

The analysis of serum samples was carried out using a simplified method, previously described for the analysis of human serum [27, 34]. The direct transesterification of the serum samples was successfully carried out at room temperature in the presence of 0.4 M KOH–CH_3OH solution. The procedure was optimized by spiking 100 µL of serum sample with KOH methanolic solution at various concentrations (KOH-CH_3OH 0.1 M, 0.2 and 0.4 M) and evaluating the reaction yield at different times. Maximum derivatization was obtained using the 0.4 M KOH methanolic solution at room temperature after 10 min. At lower KOH concentration, the FAME obtained were about 80 % of those obtained using 0.4 M KOH methanolic solution. Different quantities of serum (100, 50, 10 µl) were also tested. The RSD calculated from the peak area were used for the derivatization estimation. The RSD for 100 µl serum sample were less than 15 % while the RSD values detected for small volumes (50, 10 µl) were larger than 20 %. Additionally 100 µl produced good recoveries of FA standards at all three concentrations tested and inter-sample reproducibility was between 80 and 110 %.

In this work, a SPTM-2380 capillary column was used for GC analysis. This highly polar cyanosiloxane column was selected because its high separation efficiency of geometric (*cis*/*trans*) FAME isomers. The chromatographic separation and the subsequent analysis with EI-MS was optimized using a 37 component FAME standard mixture by modifying various parameters. Split ratios ranging from 10:1 to 100:1 and injector temperatures from 100 to 250 °C were tested. To achieve the best possible separation the temperature program of the column was also optimized using different temperature gradients. The trap, manifold and transfer line temperatures were also tested at different values with the aim of achieving the maximum stability of the polyunsaturated fatty acids at the detector. The temperature ranges studied were from 40 to 90 °C for the manifold and from 130 to 260 °C for trap and transfer line. The optimum conditions are shown under the previous section of this paper.

GC-EI-MS Analysis of FAME

For GC–MS analysis data acquisition was performed in the range *m*/*z* 50–650 in full scan mode. Figure 1 and 2 show representative GC–MS chromatograms (TIC) obtained from serum and brain of control and twitcher mice at 30 PND. Identification of the chromatographic peaks was made by comparison of the mass spectra and retention times with those provided by the FAME standards. A comparison with National Institute of Standards and Technology (NIST) library was also performed.

Saturated fatty acids could be easily identified. Their spectra were characterized by the presence of the base peak at *m*/*z* 74 $[CH_2C(OH)OCH_3]^+$ caused by McLafferty rearrangement [36]. The *m*/*z* 55 was the most abundant ion present in the MS spectra of the monounsaturated acids. The *m*/*z* 67 and *m*/*z* 79 ions were dominant in the spectra of methylene-interrupted (MI) dienes and of fatty acids with three or more MI double bonds, respectively [37]. Ethers and dimethyl acetals (DMA), already reported by other authors in humans [30, 38], were also detected and

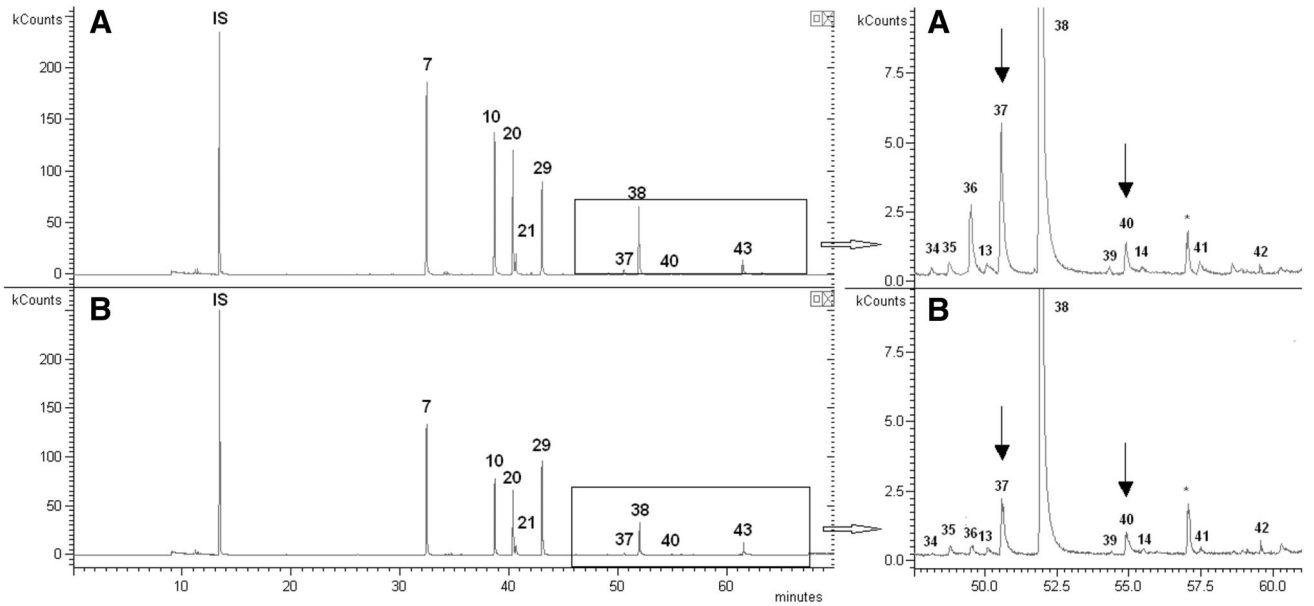

Fig. 1 Representative GC–MS chromatograms (TIC) from serum of control (**a**) and twitcher (**b**) mice at 30 PND. *IS* internal standard, *7* C16:0, *10* C18:0, *20* C18:1n9c, *21* C18:1n7c, *29* C18:2n6cc, *34* C20:2n6, *35* C20:n6c, *36* C20:3n9, *13* C22:0, *37* C20:3n6c, *38* C20:4n6, *39* C22:2n6, *40* C20:5n3c, *14* C24:0, *41* C22:4n6c, *42* C22:6, *43* C22:6n3c, *asterisk* cholesterol derivates

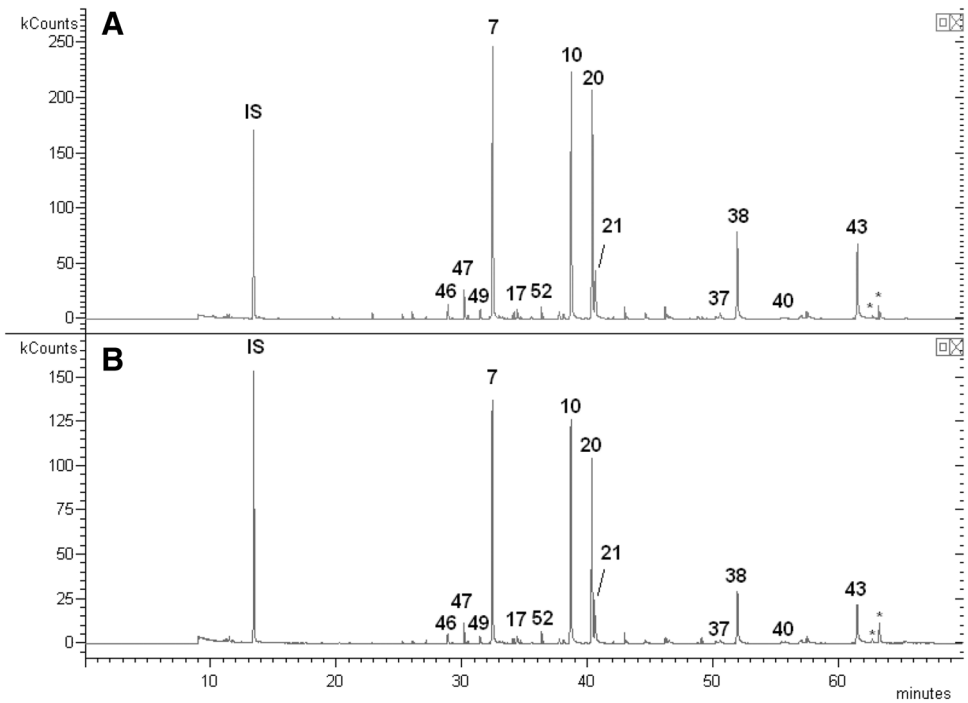

Fig. 2 Representative GC–MS chromatograms (TIC) from brain of control (**a**) and twitcher (**b**) mice at 30 PND. *IS* internal standard, *46* C18:1 ether, *47* C16:0 DMA, *49* C18:0 DMA, *7* C16:0, *17* C16:1n7c, *52* C18:1 DMA, *10* C18:0, *20* C18:1n9c, *21* C18:1n7c, *37* C20:3n6c, *38* C20:4n6, *40* C20:5n3c, *43* C22:6n3c, *asterisk* cholesterol derivates

assigned by comparing their spectra with those reported in the NIST library (*m*/*z* 71 and *m*/*z* 75 were the base peaks for ethers and DMA, respectively).

The identification of the position and of the geometry of the double bonds was also carried out. The position of the first double bond counted from the methyl end of the carbon chain was assigned when diagnostic ions with molecular formula $[C_{n+5}H_{2n+6}]^+$ were detected in the spectrum (*n* is the number of carbons from the methyl end to the first double bond), as previously asserted by other authors [37]. The *m*/*z* 108, *m*/*z* 150 and *m*/*z* 192 ions were the most abundant ions in the n-3, n-6 and n-9 families, respectively [37]. The capillary column used in this study results in a good separation of the *cis* and *trans* isomers, but

Table 1 Formula (C*a*:*b* nX z), MW, retention times and *m*/*z* base peak for each identified compound

Peak number	Compound	MW	Rt (min)	Base peak (*m*/*z*)
Saturated				
1	C10:0	186	15.37	74
2	C12:0	214	20.24	74
3	C13:0	228	23.09	74
4	C14:0	242	26.1	74
5	C15:0	257	29.23	74
6	C16:0 iso	270	30.8	74
7	C16:0	270	32.47	74
8	C17:0	284	35.56	74
9	C18:0 iso	298	37.12	74
10	C18:0	298	38.73	74
11	C19:0	312	41.69	74
12	C20:0	326	44.6	74
13	C22:0	354	50.22	74
14	C24:0	382	55.47	74
Monounsaturated				
15	C16:1	268	33.64	55
16	C16:1n9c	268	34.01	55
17	C16:1n7c	268	34.43	55
18	C18:1n9t	296	39.83	55
19	C18:1n10t	296	40.05	55
20	C18:1n9c	296	40.39	55
21	C18:1n7c	296	40.61	55
22	C20:1n9c	324	46.07	55
23	C20:1n7c	324	46.51	55
24	C22:1n9c	352	51.75	55
25	C24:1n9	380	56.92	55
Polyunsaturated				
26	C18:2n6tt	294	41.96	67
27	C18:2n6ct	294	42.42	67
28	C18:2n6tc	294	42.72	67
29	C18:2n6 cc	294	43.06	67
30	C18:3n6c	292	44.94	67
31	C18:3n3c	292	46.07	79
32	C18:3n3	292	46.07	79
33	C18:3n3	292	46.5	79
34	C20:2n6	322	48.11	67
35	C20:2n6c	322	48.76	67
36	C20:3n9	320	49.51	79
37	C20:3n6c	320	50.55	79
38	C20:4n6	318	51.96	79
39	C22:2n6	350	54.17	67
40	C20:5n3c	316	54.90	79
41	C22:4n6c	346	57.47	79
42	C22:6	342	58.61	79
43	C22:6n3c	342	61.47	79
Plasmalogen derivates				
44	C16:1 ether	254	22.91	71
45	C16:1 ether	254	25.28	71
46	C18:1 ether	282	28.88	71
47	C16:0 DMA	286	30.22	75
48	C16:1 DMA	284	30.52	75
49	C18:0 DMA	314	31.44	75
50	C18:1 DMA	312	32.99	75
51	C18:1 DMA	312	33.25	75
52	C18:1 DMA	314	36.41	75
53	C18:1 DMA	312	37.77	75
54	C18:1 DMA	312	38.11	75

For C*a*:*b* nX z formula see the "Results" section

not all positional isomers are completely separated and identified. A good chromatographic separation was obtained in any case for the all *trans* isomers which were well separated from the all *cis* isomers. Additionally, we found that for each investigated PUFA the isomers with one *cis* and one *trans* double bond were positioned between the all *cis* and all *trans* isomers. The complexity of the sample separation emerged in the chromatographic segment from 37 to 57 min, in which the unsaturated C18 FAME, C20 FAME and C22 FAME eluted. Not all C18:3 isomers were entirely separated and a partial coelution with C20:1 isomers was detected. The partial overlap of some isomers did not help the assignation of the relative peaks, so that the selected ion monitoring was performed to help the separation and the identification of these species. In addition, the qualitative identification of little peaks was significantly influenced by noise, so that in many cases their identity was successfully recognized after background subtracting. Differences in the spectra of *cis* and *trans* MUFA were not found and similar difficulties were also found for some PUFA. However, the attribution of the position and of the geometry of the double bonds of many unsaturated FAME was successfully carried out by the comparison with the MS spectra and retention times of the available standard, with NIST library and also on the basis of chromatographic elution data provided in the literature when the same stationary phase was employed [27].

The identified compounds are listed in Table 1. The presence of 54 FA was detected including 14 saturated FA, 11 MUFA and 18 PUFA. The presence of plasmalogen derivates (C16:1 DMA, C18:0 DMA, C18:1 DMA, etc.) was detected in the all analyzed brain samples, while their presence in the serum was often not detectable. In the Table 1 the FA are abbreviated using the formula, C*a*:*b* nX z. In the formula *a* is the number of carbon atoms in the fatty acid chain, *b* is the number of double bonds, nX is the location of the double bond on the Xth carbon–carbon bond, counting from the terminal methyl carbon towards the carbonyl carbon group and z is the geometrical

Table 2 FA percentage composition of brain samples ($n = 16$)

Compound	Control group		Twitcher group		ANOVA		
	20–29 days old ($n = 8$)	30–40 days old ($n = 8$)	20–29 days old ($n = 8$)	30–40 days old ($n = 8$)	Age	Disease	*X*
Saturated							
C12:0	–	–	–	–			
C14:0	0.623 ± 0.150	0.418 ± 0.173	0.712 ± 0.127	0.460 ± 0.109	0.0001	NS	
C15:0	–	–	0.113 ± 0.063	0.105 ± 0.051	NS	NS	
C16:0	24.849 ± 1.694	24.125 ± 1.139	25.930 ± 1.219	25.375 ± 1.174	NS	0.0142	
C17:0	0.574 ± 0.193	0.276 ± 0.065	0.247 ± 0.101	0.216 ± 0.026	NS	NS	
C18:0	23.572 ± 1.830	23.571 ± 0.963	23.401 ± 1.110	24.185 ± 1.474	NS	NS	
C20:0	0.637 ± 0.232	0.602 ± 0.143	0.578 ± 0.154	0.443 ± 0.009	NS	NS	
Total	50.505 ± 2.650	49.199 ± 1.992	51.084 ± 1.799	50.842 ± 2.186	0.0022	NS	
Monounsaturated							
C16:1	–	–	0.101 ± 0.028	0.116 ± 0.016	NS	NS	
C16:1n9c	–	0.292 ± 0.062	–	0.414 ± 0.046		0.0004	
C16:1n7c	0.771 ± 0.104	0.663 ± 0.112	0.867 ± 0.095	0.850 ± 0.073	NS	0.0002	
C18:1n9t	0.190 ± 0.034	0.291 ± 0.083	0.060 ± 0.010	0.089 ± 0.022	NS	NS	
C18:1n9c	16.049 ± 1.265	17.181 ± 0.907	16.421 ± 0.582	17.152 ± 0.557	0.0032	NS	
C18:1n7c	4.704 ± 0.450	5.232 ± 0.436	5.029 ± 0.301	5.343 ± 0.312	0.0033	NS	
C20:1n9c	1.066 ± 0.327	1.533 ± 0.310	0.880 ± 0.192	0.962 ± 0.203	0.0054	0.0003	0.0434
C20:1n7c	0.439 ± 0.178	0.612 ± 0.102	0.340 ± 0.038	0.312 ± 0.063	NS	0.0005	
Total	23.695 ± 1.815	25.94 ± 1.509	24.108 ± 1.042	25.215 ± 1.082	NS	NS	
Polyunsaturated							
C18:2n6ct	0.388 ± 0.060	0.245 ± 0.051	0.018 ± 0.003	0.040 ± 0.007	NS	0.0337	
C18:2n6 cc	0.902 ± 0.141	1.108 ± 0.256	0.933 ± 0.168	0.878 ± 0.167	NS	NS	
C18:3n6c	–	–	–	–			
C20:2n6	–	–	0.117 ± 0.071	0.109 ± 0.085	NS	NS	
C20:2n6c	0.509 ± 0.087	0.378 ± 0.137	0.465 ± 0.009	0.379 ± 0.119	0.0122	NS	
C20:3n9	–	–	–	–			
C20:3n6c	0.528 ± 0.091	0.370 ± 0.143	0.448 ± 0.093	0.345 ± 0.063	0.0012	NS	
C20:4n6	8.313 ± 0.326	7.536 ± 0.760	8.678 ± 0.443	8.108 ± 0.709	0.0044	0.0403	NS
C20:5n3c	–	–	–	–			
C22:4n6c	1.145 ± 0.168	1.143 ± 0.194	1.024 ± 0.105	0.910 ± 0.290	NS	0.0225	
C22:6	0.102 ± 0.011	0.114 ± 0.017	0.104 ± 0.010	0.110 ± 0.010	NS	NS	
C22:6n3c	7.523 ± 0.948	6.858 ± 1.349	6.958 ± 1.113	6.463 ± 1.792	NS	NS	
Total	19.412 ± 1.324	18.040 ± 2.906	18.821 ± 1.654	17.445 ± 2.312	NS	NS	
Plasmalogen der.							
C16:1 ether	0.648 ± 0.116	0.470 ± 0.171	0.474 ± 0.101	0.495 ± 0.110	NS	NS	
C16:1 ether	0.250 ± 0.031	0.548 ± 0.016	0.325 ± 0.098	0.357 ± 0.095	NS	NS	
C18:1 ether	0.855 ± 0.363	1.184 ± 0.410	0.927 ± 0.154	1.142 ± 0.225	0.0164	NS	
C16:0 DMA	1.634 ± 0.311	1.780 ± 0.205	1.670 ± 0.196	1.639 ± 0.252	NS	NS	
C16:1 DMA	0.195 ± 0.096	0.293 ± 0.126	0.210 ± 0.057	0.279 ± 0.055	0.0128	NS	
C18:0 DMA	0.605 ± 0.205	0.897 ± 0.374	0.740 ± 0.139	0.903 ± 0.213	0.0183	NS	
C18:1 DMA	0.160 ± 0.056	0.217 ± 0.090	0.179 ± 0.051	0.213 ± 0.060	NS	NS	
C18:1 DMA	0.129 ± 0.049	0.215 ± 0.071	0.136 ± 0.044	0.191 ± 0.040	0.0008	NS	
C18:1 DMA	1.127 ± 0.236	1.182 ± 0.274	1.002 ± 0.148	1.006 ± 0.330	NS	0.0300	
C18:1 DMA	0.470 ± 0.127	0.416 ± 0.081	0.336 ± 0.091	0.318 ± 0.067	NS	NS	
C18:1 DMA	0.339 ± 0.128	0.370 ± 0.008	0.311 ± 0.083	0.304 ± 0.166	NS	NS	

'' – ''not detected or < 0.10 %, *NS* not statistically significant, *X* interaction for the experimental factors (age and disease)

p values ≤ 0.05 were statistically significant

Table 3 FA % composition of serum samples ($n = 16$)

Compound	Control group		Twitcher group		ANOVA		
	2029 days old ($n = 8$)	30–40 days old ($n = 8$)	20–29 days old ($n = 8$)	30–40 days old ($n = 8$)	Age	Disease	*X*
Saturated							
C12:0	0.270 ± 0.099	0.289 ± 0.068	0.277 ± 0.055	0.224 ± 0.035	NS	NS	
C14:0	1.016 ± 0.565	0.565 ± 0.150	0.966 ± 0.518	0.402 ± 0.157	0.0053	NS	
C15:0	0.150 ± 0.045	0.135 ± 0.039	0.196 ± 0.049	0.145 ± 0.033	NS	NS	
C16:0	28.816 ± 0.882	28.703 ± 2.276	31.320 ± 2.353	39.387 ± 1.568	NS	NS	
C17:0	0.492 ± 0.042	0.366 ± 0.075	0.465 ± 0.162	0.432 ± 0.112	NS	NS	
C18:0	16.372 ± 2.521	14.786 ± 3.678	14.899 ± 3.350	15.385 ± 1.081	NS	NS	
C19:0	0.108 ± 0.058	0.088 ± 0.049	0.130 ± 0.051	0.139 ± 0.069	NS	NS	
C20:0	–	–	–	–			
Total	47.657 ± 2.260	44.710 ± 3.199	48.253 ± 4.669	46.114 ± 2.208	0.0281	NS	
Monounsaturated							
C16:1	–	–	–	0.103 ± 0.012	NS	NS	
C16:1n9c	0.308 ± 0.094	0.379 ± 0.152	0.360 ± 0.063	0.385 ± 0.182	NS	NS	
C16:1n7c	0.882 ± 0.420	1.910 ± 0.780	0.754 ± 0.315	1.434 ± 0.433	0.0000	NS	
C18:1n9t	0.082 ± 0.051	0.116 ± 0.106	0.073 ± 0.035	0.166 ± 0.047	0.0114	NS	
C18:1n9c	11.014 ± 2.846	17.161 ± 4.883	11.829 ± 1.477	15.094 ± 1.461	0.0000	NS	
C18:1n7c	2.119 ± 0.287	2.970 ± 0.624	2.450 ± 0.378	2.852 ± 0.343	0.0001	NS	
C20:1n9c	0.680 ± 0.241	0.640 ± 0.229	0.676 ± 0.123	0.451 ± 0.107	NS	NS	
C20:1n7c	–	–	–	–			
Total	15.085 ± 3.538	23.178 ± 5.666	16.140 ± 1.579	20.491 ± 2.210	0.0000	NS	
Polyunsaturated							
C18:2n6ct	–	–	–	–			
C18:2n6 cc	25.542 ± 1.948	20.860 ± 3.786	22.710 ± 6.134	21.328 ± 1.445	0.0184	NS	
C18:3n6c	0.152 ± 0.045	0.130 ± 0.059	–	0.113 ± 0.048	NS	NS	
C20:2n6c	0.070 ± 0.002	0.184 ± 0.023	0.049 ± 0.008	0.123 ± 0.085	0.0426	NS	
C20:3n9	0.390 ± 0.058	0.250 ± 0.052	0.192 ± 0.059	0.097 ± 0.058	NS	NS	
C20:3n6c	0.955 ± 0.309	0.839 ± 0.240	0.445 ± 0.330	0.625 ± 0.158	NS	0.0002	
C20:4n6	6.930 ± 1.267	5.786 ± 2.536	8.114 ± 1.133	7.303 ± 1.375	NS	NS	
C20:5n3c	0.737 ± 0.145	0.534 ± 0.196	0.473 ± 0.228	0.265 ± 0.131	0.0019	0.0001	
C22:4n6c	–	–	–	–			
C22:6	0.100 ± 0.013	–	0.106 ± 0.026	–			
C22:6n3c	1.977 ± 0.630	2.846 ± 0.938	3.043 ± 0.557	3.189 ± 0.822	NS	0.0116	
Total	36.862 ± 2.685	31.428 ± 3.360	35.135 ± 4.383	33.042 ± 1.781	0.0009	NS	

'' – '' not detected or <0.10 %, *NS* not statistically significant, *X* interaction for the experimental factors (age and disease)

p values ≤ 0.05 were statistically significant

configuration (*c* for *cis* and *t* for *trans*). The term "iso" is used when a methyl branching at the second carbon (starting from the methyl terminal) is detected. The DMA abbreviation refers to dimethyl acetal.

FA Composition of Brain and Serum

The quantitative analysis of brain and serum samples was carried out using the analytical procedure described in the previous section of this paper. The results are reported in Table 2, expressed as mean percentages obtained after normalizing the relative peak areas to that of IS. A multifactor analysis of variance (two-way ANOVA) was carried out to test the significance of the observed differences. The two-way ANOVA was performed using the mouse age and the disease as experimental factors. In addition, their possible significant interactions were also tested. For each group (twitcher mouse group and control mouse group) 16 samples were collected and analyzed. The study was carried out on serum and brain samples collected from each group at various ages. The mice can be grouped in two postnatal day groups: 20–29 and 30–40 day old mice (8 animals/age group).

In the brain of twitcher mice, we found the mean percentage composition reported in Table 2: total saturated FA ranging from 50.842 to 51.084 %, total MUFA ranging from 24.108 to 25.125 % and total PUFA ranging from 17.125 to 18.526. Similar FA composition was detected in the brain of control mice, with some statistically significant differences. The most abundant saturated fatty acid was palmitic acid (C16:0) with mean values significantly increased in the brain samples obtained from twitcher mice ($p = 0.0142$). We found that the myristic acid (C14:0) content depended on the mouse age and was significantly decreased in the 30–40 day old groups. In addition, Table 2 shows that the total amount of the saturated FA was affected by the age with significantly decreased values in the 30–40 day old groups.

The C18:1n9cis and C18:1n7cis were the most abundant MUFA and their levels were affected by the mouse age ($p = 0.0032$ and $p = 0.0033$ respectively). The C16:1n7c and C16:1n9c contents were significantly higher in the twitcher brain samples ($p = 0.0002$ and $p = 0.0004$ respectively). The n-7 and n-9 eicosenoic acid (C20:1n9c and C20:1n7c) contents significantly decreased in the affected mice compared to wild type ($p = 0.0003$, $p = 0.0005$). Additionally, the two-way ANOVA analysis showed that the C20:1n9c content was significantly influenced by both the selected experimental factors and that their interaction was statistically significant ($p = 0.0434$).

The most abundant PUFA was the arachidonic acid (C20:4n6) and we found that its content decreased significantly with age ($p = 0.0044$). Additionally, arachidonic acid was found to be significantly increased in the samples from twitcher mice compared to controls ($p = 0.0403$). A significant decrease in the brain of twitcher mice compared to controls was found for docosatetraenoic acid (C22:4n6c, $p = 0.0225$). Brain plasmalogens, C18:1ether, C16:1DMA, C18:0DMA and C18:1DMA significantly increased with age in both normal and affected mice. In the affected mice only one of the C18:1DMA shows a significant decrease ($p = 0.03$).

In the serum of twitcher mice we found the following mean percentage composition (Table 3): total saturated FA ranging from 46.114 to 48.253 %, total MUFA ranging from 16.140 to 20.382 % and total PUFA ranging from 33.042 to 35.125 % in twitcher mice. As the Table 3 shows, the total saturated FA and the total PUFA levels decreased significantly in the 30–40 day old group ($p = 0.0281$ and $p = 0.0008$ respectively), while the total MUFA contents were significantly increased ($p = 0.0000$). The two-way ANOVA showed that the C20 PUFA (C20:3n6c and C20:5n3c) and the C22 PUFA (C22:6n3c) were significantly correlated with the disease. The docosahexaenoic acid (C22:6n3c) content was significantly increased in the serum of affected mice ($p = 0.0116$), but not relation with age was found. On the other and the C20 PUFA were significantly decreased in twitcher compared to wild type, with the C20:5n3c also decreased in relation to the age ($p = 0.0019$). It is important to point out that when the percentage contents of the C20:3n6c *versus* C20:5n3c percentage contents were plotted a complete separation of the two groups was observed (Fig. 3).

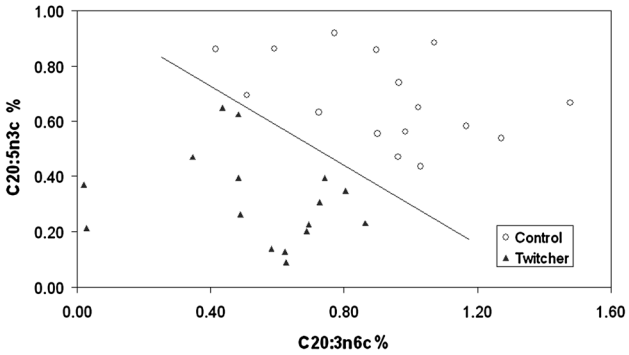

Fig. 3 C20:3n6c percentage contents plotted versus C20:5n3c percentage contents measured in the serum of control and twitcher mice

Discussion

In the present study, analytical methods conventionally employed for FA analysis in biological samples were partly modified and successfully used for brain and serum analysis [25, 32–34]. The chromatographic peaks were identified by comparison of their retention times and mass spectra with those provided by the FAME standards. The MS spectra obtained for saturated, monounsaturated and polyunsaturated fatty acids were in accordance with previously published data [25, 35–37].

Comparison of total ion content (TIC) chromatograms obtained from the GC-EI-MS analysis of control and twitcher mice revealed similar profiles. The identities of the main peaks were conserved so that qualitative changes were not detected between the two groups. Additionally, we found that the FAME profiles obtained from serum and brain sample analysis were essentially identical with some qualitative differences detected for minor components (unknown compounds).

The quantitative analysis of the identified FA was also performed. In a preliminary step, the FA percentage composition of brain and serum samples was carried out by GC-FID analysis. GC-FID is a robust analytical technique largely employed for the FAME analysis because guarantees sensitive and reproducible results. However, FID analysis is inadequate for identification purposes. In this study, the quantitative results obtained by FID was compared with those obtained by MS analysis. As other authors have previously reported [39], we did not found significant

differences (data not shown), so that GC–MS analysis was preferred and used also for quantitative aims.

The quantitative analysis revealed a similar FA composition in the brain of twitcher and control mice, with some statistically significant differences. The most abundant saturated fatty acid was the palmitic acid (C16:0) with mean values significantly increased in the twitcher brain samples. The results suggested that MUFA percentage composition was correlated with the disease. Significant differences were found for the C16:1n7c and C16:1n9c contents which were significantly increased in the twitcher brain samples. This increase is most likely due to the considerable neuroinflammation present in the brain of affected mice [40], since it has been demonstrated a positive association of palmitoleic acid with markers of inflammation [41]. Similar results were obtained for the arachidonic acid (C20:4n6) which was found to be significantly increased in the twitcher mice. This result is consistent with previously published data demonstrating that in twitcher mice the oligodendrocyte apoptotic death, induced by psychosine, is mediated by the reactive oxygen species generated by the release of arachidonic acid [42]. The observation that an abnormal FA composition may have a role in myelin abnormalities in the brain is supported by the evidence that alteration in the PUFA content is correlated to brain pathologies [18, 19]. We found also that a plasmalogen derivate (C18:1DMA) was significantly decreased in the affected mice, consistent with the observation that psychosine induces a reduction of brain plasmalogens concentration [43]. Similar results were previously obtained by other authors who found that the plasmalogen contents were decreased in Zellweger's syndrome [22].

We found also that the brain FA composition was affected by the age of the mouse. It was of great interest to verify that the arachidonic acid (C20:4n6) decreased significantly with age. This result confirmed previous results showing the effect of the age on the rat fatty acid composition [44]. These authors found that the C20:4n6 levels decreased with age and that these changes were largely compensated by the increases in C18:1n9. The total amount of the saturated FA was significantly decreased in the 30–40 day old groups while many plasmalogens were significantly increased. Additionally, we found that the C20:1n9c content was significantly influenced by both the selected experimental factors and that their interaction was statistically significant.

The results showed that the total serum FA contents were not significantly different between the two groups, but were significantly affected by the age of the mouse. The differences in the MUFA composition were only related to the age but not to the disease, unlikely with what is was observed in the brain. The total saturated FA and the total PUFA levels had decreased significantly in the 30–40 day old group, while the total MUFA contents had significantly increased. The C20:3n6c, C20:5n3c and the C22:6n3c were correlated with the disease. The C20 PUFA were significantly decreased in twitcher mice, while the C20:5n3c was increased.

To our knowledge this is the first study to provide comparative data on the distribution of fatty acids between the serum and the brain of twitcher mice. The results have highlighted, among other things, that these FA are the compounds with the greatest potential as biomarkers of Krabbe disease. It is possible that the alterations in their composition could reflect underlying metabolic changes taking place during disease progression. Further work will be required to address the relevance of reduced levels of these FA in the pathology of Krabbe disease.

Acknowledgments This study was supported by funds to Alice Luddi from the Tuscany Region "Bando salute 2009".

References

1. Suzuki K, Suzuki Y (1970) Globoid cell leucodystrophy (Krabbe's disease): deficiency of galactocerebroside beta-galactosidase. Proc Natl Acad Sci USA 66:302–309
2. Vanier MT, Svennerholm L (1975) Chemical pathology of Krabbe's disease. III. Ceramide-hexosides and gangliosides of brain. Acta Paediatr Scand 64:641–648
3. Svennerholm L, Vanier MT, Mansson JE (1980) Krabbe disease: a galactosylsphingosine (psychosine) lipidosis. J Lipid Res 21:53–64
4. Nagara H, Ogawa H, Sato Y, Kobayashi T, Suzuki K (1986) The twitcher mouse: degeneration of oligodendrocytes in vitro. Brain Res 391:79–84
5. Tanaka K, Nagara H, Kobayashi T, Goto I (1988) The twitcher mouse: accumulation of galactosylsphingosine and pathology of the sciatic nerve. Brain Res 454:340–346
6. Rafi MA, Rao HZ, Luzi P, Curtis MT, Wenger DA (2012) Extended normal life after AAVrh10-mediated gene therapy in the mouse model of Krabbe disease. Mol Ther 20:2031–2042
7. Luddi A, Volterrani M, Strazza M, Smorlesi A, Rafi MA, Datto J, Wenger DA, Costantino-Ceccarini E (2001) Retrovirus-mediated gene transfer and galactocerebrosidase uptake into twitcher glial cells results in appropriate localization and phenotype correction. Neurobiol Dis 8:600–610
8. Costantino-Ceccarini E, Luddi A, Volterrani M, Strazza M, Rafi MA, Wenger DA (1999) Transduction of cultured oligodendrocytes from normal and twitcher mice by a retroviral vector containing human galactocerebrosidase (GALC) cDNA. Neurochem Res 24:287–293
9. Caniglia M, Rana I, Pinto RM, Fariello G, Caruso R, Angioni A, Dionisi Vici C, Sabetta G, De Rossi G (2002) Allogeneic bone marrow transplantation for infantile globoid-cell leukodystrophy (Krabbe's disease). Pediatr Transplant 6:427–431
10. Lim ZY, Ho AY, Abrahams S, Fensom A, Aldouri M, Pagliuca A, Shaw C, Mufti GJ (2008) Sustained neurological improvement following reduced-intensity conditioning allogeneic haematopoietic stem cell transplantation for late-onset Krabbe disease. Bone Marrow Transpl 41:831–832
11. Claudino WM, Quattrone A, Biganzoli L, Pestrin M, Bertini I, Di Leo A (2007) Metabolomics: available results, current research

projects in breast cancer, and future applications. J Clin Oncol 25:2840–2846
12. Wikoff WR, Gangoiti JA, Barshop BA, Siuzdak G (2007) Metabolomics identifies perturbations in human disorders of propionate metabolism. Clin Chem 53:2169–2176
13. Bogdanov M, Matson WR, Wang L, Matson T, Saunders-Pullman R, Bressman SS, Flint Beal M (2008) Metabolomic profiling to develop blood biomarkers for Parkinson's disease. Brain 131:389–396
14. Deo RC, Hunter L, Lewis GD, Pare G, Vasan RS, Chasman D, Wang TJ, Gerszten RE, Roth FP (2010) Interpreting metabolomic profiles using unbiased pathway models. PLoS Comput Biol 6:e1000692
15. Fiehn O (2001) Combining genomics, metabolome analysis, and biochemical modelling to understand metabolic networks. Comp Funct Genomics 2:155–168
16. O'Brien JS, Sampson EL (1965) Lipid composition of the normal human brain: gray matter, white matter, and myelin. J Lipid Res 6:537–544
17. O'Brien JS, Sampson EL (1965) Fatty acid and fatty aldehyde composition of the major brain lipids in normal human gray matter, white matter, and myelin. J Lipid Res 6:545–551
18. Hooijmans CR, Kiliaan AJ (2008) Fatty acids, lipid metabolism and Alzheimer pathology. Eur J Pharmacol 585:176–196
19. Vanier MT (1999) Lipid changes in Niemann-Pick disease type C brain: personal experience and review of the literature. Neurochem Res 24:481–489
20. Martinez M (1986) Myelin in the developing human cerebrum. Brain Res 364:220–232
21. Heymans HS, Schutgens RB, Tan R, van den Bosch H, Borst P (1983) Severe plasmalogen deficiency in tissues of infants without peroxisomes (Zellweger syndrome). Nature 306:69–70
22. Martinez M, Ichaso N, Setien F, Durany N, Qiu X, Roesler W (2010) The Delta4-desaturation pathway for DHA biosynthesis is operative in the human species: differences between normal controls and children with the Zellweger syndrome. Lipids Health Dis 9:98
23. Igisu H, Shimomura K, Kishimoto Y, Suzuki K (1983) Lipids of developing brain of twitcher mouse. An authentic murine model of human Krabbe disease. Brain 106(2):405–417
24. Esch SW, Williams TD, Biswas S, Chakrabarty A, LeVine SM (2003) Sphingolipid profile in the CNS of the twitcher (globoid cell leukodystrophy) mouse: a lipidomics approach. Cell Mol Biol (Noisy-le-grand) 49:779–787
25. Araujo P, Nguyen TT, Froyland L, Wang J, Kang JX (2008) Evaluation of a rapid method for the quantitative analysis of fatty acids in various matrices. J Chromatogr A 1212:106–113
26. Eder K (1995) Gas chromatographic analysis of fatty acid methyl esters. J Chromatogr B Biomed Appl 671:113–131
27. Sanchez-Avila N, Mata-Granados JM, Ruiz-Jimenez J, Luque de Castro MD (2009) Fast, sensitive and highly discriminant gas chromatography-mass spectrometry method for profiling analysis of fatty acids in serum. J Chromatogr A 1216:6864–6872
28. Kimura M, Yoon HR, Wasant P, Takahashi Y, Yamaguchi S (2002) A sensitive and simplified method to analyze free fatty acids in children with mitochondrial beta oxidation disorders using gas chromatography/mass spectrometry and dried blood spots. Clin Chim Acta 316:117–121
29. Aleryani SL, Cluette-Brown JE, Khan ZA, Hasaba H, Lopez de Heredia L, Laposata M (2005) Fatty acid methyl esters are detectable in the plasma and their presence correlates with liver dysfunction. Clin Chim Acta 359:141–149
30. Bicalho B, David F, Rumplel K, Kindt E, Sandra P (2008) Creating a fatty acid methyl ester database for lipid profiling in a single drop of human blood using high resolution capillary gas chromatography and mass spectrometry. J Chromatogr A 1211:120–128
31. Sakai N, Inui K, Tatsumi N, Fukushima H, Nishigaki T, Taniike M, Nishimoto J, Tsukamoto H, Yanagihara I, Ozono K, Okada S (1996) Molecular cloning and expression of cDNA for murine galactocerebrosidase and mutation analysis of the twitcher mouse, a model of Krabbe's disease. J Neurochem 66:1118–1124
32. Bligh EG, Dyer WJ (1959) A rapid method of total lipid extraction and purification. Can J Biochem Physiol 37:911–917
33. Morrison WR, Smith LM (1964) Preparation of fatty acid methyl esters and dimethylacetals from lipids with boron fluoride-methanol. J Lipid Res 5:600–608
34. Yi L, He J, Liang Y, Yuan D, Gao H, Zhou H (2007) Simultaneously quantitative measurement of comprehensive profiles of esterified and non-esterified fatty acid in plasma of type 2 diabetic patients. Chem Phys Lipids 150:204–216
35. Carlson LA (1985) Extraction of lipids from human whole serum and lipoproteins and from rat liver tissue with methylene chloride-methanol: a comparison with extraction with chloroform–methanol. Clin Chim Acta 149:89–93
36. McLafferty FW (1959) Molecular rearrangements. Anal Chem 31:82–87
37. Mjos SA, Pattersen J (2003) Determination of trans double bonds in polyunsaturated fatty acid methyl esters from their electron impact mass spectra. Eur J Lipid Sci Technol 105:156–164
38. Masood A, Stark KD, Salem N Jr (2005) A simplified and efficient method for the analysis of fatty acid methyl esters suitable for large clinical studies. J Lipid Res 46:2299–2305
39. Dodds ED, McCoy MR, Rea LD, Kennish JM (2005) Gas chromatographic quantification of fatty acid methyl esters: flame ionization detection vs. electron impact mass spectrometry. Lipids 40:419–428
40. Mohri I, Taniike M, Taniguchi H, Kanekiyo T, Aritake K, Inui T, Fukumoto N, Eguchi N, Kushi A, Sasai H, Kanaoka Y, Ozono K, Narumiya S, Suzuki K, Urade Y (2006) Prostaglandin D2-mediated microglia/astrocyte interaction enhances astrogliosis and demyelination in twitcher. J Neurosci 26:4383–4393
41. Perreault M, Roke K, Badawi A, Nielsen DE, Abdelmagid SA, El-Sohemy A, Ma DW, Mutch DM (2013) Plasma levels of 14:0, 16:0, 16:1n-7, and 20:3n-6 are positively associated, but 18:0 and 18:2n-6 are inversely associated with markers of inflammation in young healthy adults. Lipids 49(3):255–263
42. Giri S, Khan M, Rattan R, Singh I, Singh AK (2006) Krabbe disease: psychosine-mediated activation of phospholipase A2 in oligodendrocyte cell death. J Lipid Res 47:1478–1492
43. Khan M, Haq E, Giri S, Singh I, Singh AK (2005) Peroxisomal participation in psychosine-mediated toxicity: implications for Krabbe's disease. J Neurosci Res 80:845–854
44. Ulmann L, Mimouni V, Roux S, Porsolt R, Poisson JP (2001) Brain and hippocampus fatty acid composition in phospholipid classes of aged-relative cognitive deficit rats. Prostaglandins Leukot Essent Fatty Acids 64:189–195